ON THE RELATIONSHIP BETWEEN THE POLE CONDITION, ABSORBING BOUNDARY CONDITIONS AND PERFECTLY MATCHED LAYERS

M. GANDER* AND A. SCHÄDLE†

Abstract. Transparent (or exact or non-reflecting) boundary conditions are essential to truncate infinite computational domains. Since transparent boundary conditions are usually non-local and expensive, they must be approximated. In this paper, we study such an approximation for the Helmholtz equation on an infinite strip, based on the pole condition. We show that a discretization of the pole condition can be interpreted both as a high order absorbing boundary condition and as a perfectly matched layer, two other well known methods for approximating a transparent boundary condition. We give an error estimate which shows exponential convergence in the absence of Wood anomalies.

Key words. transparent boundary condition, pole condition, high order absorbing boundary conditions, perfectly matched layer, exterior (complex) scaling.

AMS subject classifications. 65N15, 65N55

1. Introduction.

To simulate wave propagation in infinite domains, transparent boundary conditions are artificially introduced at the boundary of a computational domain in order to truncate the infinite domain, see the seminal papers by Engquist and Majda [13], and Bayliss and Turkel [6]. Transparent (or exact or non-reflecting) boundary conditions are by definition conditions which lead to a solution on the truncated computational domain which is identical to the solution one would obtain on the unbounded domain. For the Helmholtz equation in a waveguide for example, transparent boundary conditions were studied by Fix and Marin [15], and for more general geometries by Keller and Givoli [36]. Such conditions are in general non-local and expensive to use, and they are therefore approximated in practice, such that no too large artificial reflections are introduced, and the truncated problem can be solved efficiently. High order rational approximations of transparent boundary conditions for the Helmholtz equation are discussed in [2, 26, 27]. The high order rational approximations of [26, 27] are based on rational best approximations on certain intervals and yield much faster convergence than we will obtain here from the Pole condition, see the discussion in section 4.3.1. For a broad review on transparent boundary conditions and their approximations we refer to the review by Tsynkov [46]. For approximate transparent boundary conditions in the time-domain, especially the wave equation, we refer to the two articles by Hagstrom [24, 25]. Transparent boundary conditions and their approximations for the time-dependent Schrödinger equation are reviewed in [1].

Compared to rational approximations, a seemingly very different technique to truncate infinite domains for computations are perfectly matched layers (PML), which were introduced by Bérenger [8]. There, the idea is to surround the computational domain with a layer with different material properties, in which outgoing waves are absorbed. Bérenger's perfectly matched layer can be interpreted as a complex coordinate stretching, see [12, 19]. There is a well known connection between rational approximations and PML. Gudatti and Lim show in [21] that using linear finite elements and

*Mathematics Section, University of Geneva, CH-1211, Geneva, Switzerland

†Mathematical Institute, Faculty of Mathematics and Natural Sciences, Heinrich Heine University Düsseldorf , D-40225 Düsseldorf, Germany

midpoint quadrature to assemble the mass matrix, the PML can be interpreted as a continued fraction approximation. Earlier, Asvadurov et al constructed in [4] an optimal finite difference approximation for a PML based on rational best approximations of the square root.

Yet another technique is based on the pole condition, which was first formulated for the Helmholtz equation by Schmidt [42] and later analyzed in [33]. Using a certain Hardy space the pole condition is reformulated in [32] for the Helmholtz equation and in [40] for time-dependent partial differential equations such as the Schrödinger or wave equation. In [32] a variational framework is developed, the so called Hardy space infinite element method, which results in a discretization that is almost equivalent to the one obtained by matching moments in [40]. The pole condition was extended to certain homogeneous exterior domains [43, 38, 39] and to elastic problems [30, 29].

Our goal here is to explore relations between these techniques, in order to obtain rigorous error estimates for the Pole Condition and optimize its performance. We start in Section 2 by describing our model problem, the Helmholtz equation in a very simple geometry, an infinite strip, which we use to study in detail one possible discretization of the pole condition introduced in Section 3. There are several ways to obtain a discretization of the pole condition:

- by matching moments as in [40], which is the ansatz we use here and describe in detail in Section 3,
- by a Galerkin ansatz in Hardy space [32], which gives an almost equivalent discrete system of equations and
- by a collocation ansatz, which is currently under investigation.

We show in Section 4 that with the matching moment discretization, the pole condition can be rewritten as a truncated continued fraction. This allows us to prove that the pole condition with this discretization is nothing else than a Padé approximation of the Dirichlet to Neumann (DtN) operator. The DtN operator is the essential ingredient in a transparent boundary condition that has to be approximated to obtain a practical method. Having this interpretation of the pole condition, we can establish rigorous error estimates for the pole condition. In addition, we can also show that the pole condition with this discretization is equivalent to a complex coordinate stretching, which gives a natural relation of the pole condition to the perfectly matched layer technique.

The use of Padé approximations to obtain absorbing boundary conditions is not new. Engquist and Majda [13] already used continued fractions or Padé approximants to obtain absorbing boundary conditions for the wave equation. Thus the pole condition for this special example turns out to be closely related to the boundary conditions derived in [23], and is a high-order local absorbing boundary condition. There is a short review on these by Givoli [20]. Rational Hermite interpolation has also been used to obtain absorbing boundary conditions, see [7]. Over the last decades, absorbing boundary conditions have also become more and more important for domain decomposition methods in the context of optimized Schwarz methods [16]. Since local sub-domain solutions should be as close as possible to the global solution, sub-domains can be interpreted as truncated computational domains, leading to Schwarz methods based on domain truncation [18]. High order absorbing transmission conditions and perfectly matched layers are currently a very active field of research in domain decomposition, see [45, 41, 22, 3] for the use of perfectly matched layers, [9] for Padé approximations, the sweeping preconditioner [14], the source transfer method [10, 11], the method of Stolk [44], and the method of polarized traces [47]; for a comprehensive review, see [17] and [18].

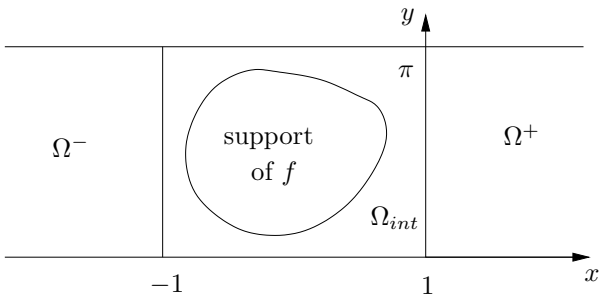

FIG. 2.1. *Domain and support of f*

2. Model Problem. In order to give a rigorous error analysis for the domain truncation technique obtained from the pole condition, we consider the Helmholtz equation on an infinite strip,

$$-(\partial_{xx}+\partial_{yy}+k^2)u(x,y)=f(x,y), \qquad (x,y)\in\Omega:=\mathbb{R}\times(0,\pi), \tag{2.1a}$$

$$u(x,0)=u(x,\pi)=0, \qquad x\in\mathbb{R}, \tag{2.1b}$$

$$u(x,y) \text{ satisfies a radiation condition for} \qquad |x|\to\infty \tag{2.1c}$$

with a real-valued wavenumber k^2, which may depend on y, and a compactly supported source f, e.g. $\mathrm{supp}(f)\subset(-1,1)\times(0,\pi)$, as indicated in Figure 2.1. Problem (2.1) has to be completed with radiation conditions at infinity. In our simple, quasi one-dimensional setting, these may be derived as follows: denote by (κ_n^2,ψ_n) the eigenpairs of the operator $\partial_{yy}+k^2$ on the Sobolev space of weakly differentiable functions $H_0^1(0,\pi)$, with generalized 0 boundary condition, and assume that k^2 is such that the eigenvalues κ_n^2 are real. For example when k^2 is constant, we obtain $\kappa_n^2=k^2-n^2$, where n^2 for $n\in\mathbb{N}$ are the eigenvalues of $-\partial_{yy}$ with homogeneous Dirichlet boundary conditions. Note that the eigenvalues and eigenfunctions (κ_n^2,ψ_n) may be different for the left and right waveguide, $\Omega^{\pm}$a. In order to keep the notation simple, we will assume however that (κ_n^2,ψ_n) are the same for Ω^+ and Ω^-. We will further assume that the eigenfunctions ψ_n are normalized and that there are no Wood anomalies, i.e. we are in the non-degenerate case such that

$$\kappa_n^2\neq 0. \tag{2.2}$$

If the operator $\partial_{yy}+k^2$ is already discretized, then there are only finitely many eigenpairs, which will also be denoted by (κ_n^2,ψ_n) . As before we will assume that the problem is non-degenerate. Since the implementation of the pole condition requires only multiplications by κ_n^2 (cf. Equations (3.7) to (3.10) below), which correspond to applications of $\partial_{yy}+k^2$ or a discretization thereof, the actual calculation of the eigenpairs is not necessary for using the pole condition truncation.

Solutions of (2.1a) and (2.1b) without source term are then

$$u(x,y)=\sum_n a_n \mathrm{e}^{i\lambda_n x}\psi_n(y)+b_n\mathrm{e}^{-i\lambda_n x}\psi_n(y), \tag{2.3}$$

where we defined $i:=\sqrt{-1}$ [1] and thus

$$i\lambda_n:=-\sqrt{-\kappa_n^2} \text{ when } \kappa_n^2\leq 0 \text{ and } i\lambda_n:=i\sqrt{\kappa_n^2} \text{ when } \kappa_n^2>0. \tag{2.4}$$

[1] For $z=r\mathrm{e}^{i\phi}\in\mathbb{C}$ with $r\geq 0$, $\phi\in(-\pi,\pi]$, we define $\sqrt{z}:=\sqrt{r}\mathrm{e}^{i\frac{\phi}{2}}$ taking the cut along the negative real axis.

When κ_n^2 is negative, $e^{i\lambda_n x}$ is exponentially decaying for $x \to \infty$, whereas $e^{-i\lambda_n x}$ grows exponentially for $x \to \infty$. When κ_n^2 is positive, $e^{\pm i\lambda_n x}$ are propagating. Taking the common time-dependency as $e^{-i\omega t}$ the mode $e^{i(\lambda_n x - \omega t)}$ is traveling to the right and $e^{i(-\lambda_n x - \omega t)}$ is traveling to the left.

As we are interested in physically meaningful solutions, we require $b_n = 0$ in (2.3) for solutions in the right exterior strip Ω^+. For solutions in the left exterior strip Ω^- we require $a_n = 0$ in (2.3).

REMARK 2.1. *The Sommerfeld radiation condition for the Helmholtz equation in* $\mathbb{R}^d$, $-\Delta u - \kappa^2 u = f$, *is* $\lim_{|x|\to\infty} |x|^{\frac{d-1}{2}}(\partial_\nu - i\kappa)u = 0$. *Thus for positive* κ_n^2 *the term* $e^{i\lambda_n x}$ *in* (2.3) *obeys the 1D Sommerfeld condition for* $x \to \infty$. *Hence our requirement is in accordance with the usual Sommerfeld radiation condition.*

If one wants to compute a numerical approximation of the solution of (2.1), one needs to truncate the infinite domain in order to obtain a computational domain of finite size, on which the equation can then be discretized and solved. One therefore needs boundary conditions, in our example at $x = -1$ and $x = 1$. The best boundary conditions possible are such that if one solves the problem on the bounded domain, one obtains the same solution as if one would have solved the problem on the unbounded domain. These boundary conditions are called transparent boundary conditions, non-reflecting boundary conditions, or exact boundary conditions. They can be obtained by considering a decomposition of the domain Ω into a computational domain $\Omega_{int} := (-1, 1) \times (0, \pi)$, and an outer domain which in our case consists of two infinite strips, $\Omega^- := (-\infty, -1) \times (0, \pi)$ on the left, and $\Omega^+ := (1, \infty) \times (0, \pi)$ on the right. Imposing continuity of the traces of the respective solutions and their normal derivatives at the artificial interfaces at $x = \pm 1$, we obtain a domain decomposition formulation which is equivalent to the original one on the unbounded domain. The idea is now to solve the problem in the outer domain exactly, since there the source term f vanishes. For our example, the problem on the semi-infinite strip on the right is

$$\begin{aligned} -(\partial_{xx} + \partial_{yy} + k^2)u(x, y) &= 0 \qquad && (x, y) \in \Omega^+, \\ u(x, 0) = u(x, \pi) &= 0 && x \in [1, \infty), \\ u(1, y) &= g(y) && y \in (0, \pi), \end{aligned} \tag{2.5}$$

with Dirichlet data g. Using the decomposition into eigenfunctions (2.3), we obtain the closed form solution

$$u(x, y) = \sum_n a_n \psi_n(y) e^{i\lambda_n(x-1)}, \tag{2.6}$$

where $a_n = \int_0^\pi g(y)\overline{\psi_n}(y)dy$ are the expansion coefficients of $g(y)$ for the normalized eigenfunctions ψ_n and $b_n = 0$ as explained above. Similarly, the outward radiating solution on the left semi-infinite strip Ω^- is

$$u(x, y) = \sum_n b_n \psi_n(y) e^{i\lambda_n(-x-1)}, \tag{2.7}$$

with b_n the expansion coefficients of the Dirichlet data at $x = -1$. This time we require $a_n = 0$ to obtain a physically meaningful solution.

Note that $\hat{u}_n(x) := a_n e^{i\lambda_n(x-1)}$ in (2.6) satisfies for any $x \in [1, \infty)$ the condition

$$\partial_x \hat{u}_n(x) - i\lambda_n \hat{u}_n(x) = 0. \tag{2.8}$$

An analogous condition holds for $x \in (-\infty, -1]$,

$$-\partial_x \hat{u}_n(x) - i\lambda_n \hat{u}_n(x) = 0. \tag{2.9}$$

Since the solution and its normal derivative need to match at the interfaces $x = \pm 1$, the solution inside the computational domain also needs to satisfy

$$\partial_\nu \hat{u}_n(x) - i\lambda_n \hat{u}_n(x) = 0 \text{ at } x = \pm 1, \tag{2.10}$$

where ∂_ν denotes the outward normal derivative for Ω_{int}. These conditions are hence the transparent boundary conditions, because the solution obtained with these conditions to truncate the domain is the same as the solution on the unbounded domain. It should be stressed that the fact that the radiation condition holds for any $|x| > 1$ and not only in the limit $x \to \infty$ is a special one dimensional feature which also holds for the quasi-one-dimensional waveguide case considered here.

We define the Dirichlet to Neumann Operator DtN for the right and left boundary by

$$\partial_\nu u(\pm 1, y) = \mathrm{DtN} u(\pm 1, y) := \sum_n i\lambda_n \underbrace{\int_0^\pi u(\pm 1, \vartheta)\overline{\psi_n(\vartheta)} d\vartheta}_{=:\hat{u}_n(\pm 1)} \psi_n(y), \tag{2.11}$$

which shows that $i\lambda_n$ in our notation is the symbol of the DtN operator. We then obtain on the bounded domain the system

$$\begin{aligned} -(\partial_{xx} + \partial_{yy} + k^2)u &= f && \text{in } \Omega_{int}, \\ u &= 0 && \text{on } [-1,1] \times \{0, \pi\}, \\ \partial_\nu u &= \mathrm{DtN} u && \text{on } \pm 1 \times (0, \pi). \end{aligned} \tag{2.12}$$

The symbols $i\lambda_n$ of the DtN operators in the transparent boundary conditions (2.10) contain square-roots of the eigenvalues κ_n^2 from the eigenfunction expansion, see (2.4), and represent therefore non-local operators along the artificial interfaces, which are expensive to evaluate in a finite difference or a finite element setting. Their discretization would lead to a dense matrix at the interfaces, and one is therefore interested in approximating the transparent boundary conditions (2.10). For this purpose the two major well established techniques are absorbing boundary conditions (ABC), where the square-root is approximated by a polynomial or rational function of κ_n^2, and perfectly matched layers (PML), where a modified equation is solved in a layer which is added to the computational domain. The pole condition truncation (PCT) is a further, more recent technique to approximate the transparent boundary condition (2.10). In what follows, we will show that the PCT is in fact a certain Padé approximation of the square root, and hence it is an ABC. On the other hand, it can also be interpreted as a special PML, with a constant stretching parameter on an equidistant grid. This shows that ABC and PML techniques are not as different as it might appear at first glance.

3. Pole Condition Truncation (PCT). To simplify the notation, we will omit the subscript n in what follows. We perform a Laplace transform in the distance q to the boundary, where $q = x - 1$ on the right exterior strip, and $q = -(x + 1)$ on the left exterior strip. Denoting the Laplace transform by $\mathcal{L}$ with dual variable s from (2.5) one obtains

$$-(s^2 + \kappa^2)\mathcal{L}(\hat{u})(s) + \partial_\nu \hat{u}(1) + s\hat{u}(1) = 0. \tag{3.1}$$

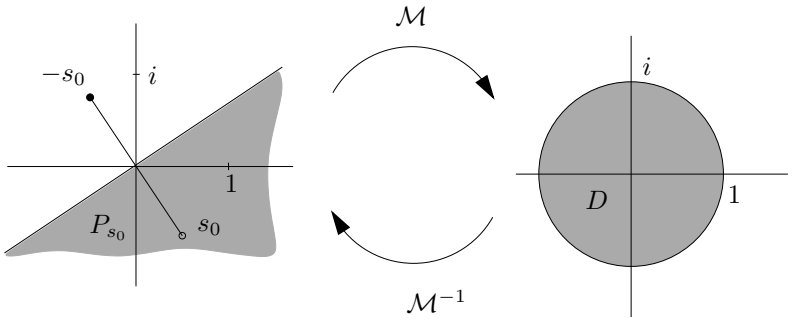

FIG. 3.1. *Sketch of the Möbius transform mapping P_{s_0} to D.*

Here $\mathcal{L}(\hat{u})(s)$, $\hat{u}(1)$ as well as $\partial_\nu \hat{u}(1)$ are functions of k^2. Solving for $\mathcal{L}(\hat{u})(s)$ and performing a partial fraction decomposition, we obtain

$$\mathcal{L}(\hat{u})(s) = \frac{\partial_\nu \hat{u}(1) + s\hat{u}(1)}{s^2+\kappa^2} = \tag{3.2}$$
$$\underbrace{\frac{1}{2}\frac{\hat{u}(1) - \frac{1}{i\lambda}\partial_\nu \hat{u}(1)}{s+i\lambda}}_{\text{incoming / exponentially increasing}} + \underbrace{\frac{1}{2}\frac{\hat{u}(1) + \frac{1}{i\lambda}\partial_\nu \hat{u}(1)}{s-i\lambda}}_{\text{outgoing / evanescent}},$$

where $\lambda = \lambda_n$ from (2.4). Therefore $\mathcal{L}(\hat{u})(s)$ has two singularities (poles), one at $s = i\lambda$ and one at $s = -i\lambda$. If we consider the problem (2.5), the transparent boundary condition (2.10) implies that $\hat{u}(1) - (i\lambda)^{-1}\partial_\nu \hat{u}(1) = 0$. Thus the first term on the right in (3.2) vanishes, and the physically meaningful solution $\mathcal{L}(\hat{u})(s)$ of (3.2) is given by

$$\mathcal{L}(\hat{u})(s) = \frac{1}{2}\frac{\hat{u}(1) + \frac{1}{i\lambda}\partial_\nu \hat{u}(1)}{s-i\lambda}. \tag{3.3}$$

Note that this way, since the inverse Laplace transform of $(s-i\lambda)^{-1}$ is $\mathrm{e}^{i\lambda q}$, u is a combination of outgoing and evanescent modes. Hence the part of $\mathcal{L}(\hat{u})(s)$ that obeys the TBC is analytic on the positive real line and on the negative imaginary axis, whereas the part of $\mathcal{L}(\hat{u})(s)$ which we wish to exclude, as it does not obey the TBC, has singularities there. The key idea of the PCT is to write the solution $\mathcal{L}(\hat{u})(s)$ explicitly as an expression which is necessarily analytic in a region of the complex plane, which contains the positive real axis and the negative imaginary axis. It is convenient to choose for the region a half space, say $P_{s_0} := \{z \in \mathbb{C} : \Re(z/s_0) > 0\}$, with $\Re s_0 > 0$ and $\Im s_0 < 0$, as shown in Figure 3.1.

Since analytic functions on a disc can be represented by a power series, we map the half space P_{s_0} using a Möbius transform onto the unit disk $D = \{z \in \mathbb{C} : |z| < 1\}$, such that the expansion point s_0 is mapped to the origin. The Möbius transform and its inverse are

$$\mathcal{M}_{s_0} : P_{s_0} \to D\ ,\ s \mapsto z := \frac{s_0 - s}{s_0 + s} \quad , \quad \mathcal{M}_{s_0}^{-1} : D \to P_{s_0}\ ,\ z \mapsto s = s_0\frac{1-z}{1+z}. \tag{3.4}$$

We now expand $\mathcal{L}(\hat{u})(s)$ into a power-series in the new variable z,

$$U(z) := \mathcal{L}(\hat{u})(s(z)) = \frac{1+z}{2s_0}\left((1+z)\sum_{\ell=0}^{\infty}\hat{a}_\ell z^\ell + \hat{u}(1)\right). \tag{3.5}$$

We choose this particular form of the power series, because the general theory of Laplace transforms implies that if the inverse transform $\hat{u}$ exists, then we must have $\lim_{s\to\infty} s\mathcal{L}(\hat{u})(s) = \hat{u}(1)$, which holds for our ansatz, because

$$\lim_{s\to\infty} s\mathcal{L}(\hat{u})(s) = \lim_{z\to -1} s_0 \frac{1-z}{1+z} U(z) = \hat{u}(1). \tag{3.6}$$

Inserting the power series (3.5) into equation (3.1), we obtain

$$-\left(s_0^2\frac{(1-z)^2}{(1+z)^2}+\kappa^2\right)\frac{(1+z)}{2s_0}\left((1+z)\sum_{\ell=0}^{\infty}\hat{a}_\ell z^\ell + \hat{u}(1)\right) + \partial_\nu \hat{u}(1) + s_0\frac{1-z}{1+z}\hat{u}(1) = 0.$$

Multiplying by -1 and rearranging terms gives

$$\left(\frac{\kappa^2+s_0^2}{2s_0} + 2\frac{\kappa^2-s_0^2}{2s_0}z + \frac{\kappa^2+s_0^2}{2s_0}z^2\right)\sum_{\ell=0}^{\infty}\hat{a}_\ell z^\ell - \partial_\nu\hat{u}(1) + \left(\frac{\kappa^2-s_0^2}{2s_0}+\frac{\kappa^2+s_0^2}{2s_0}z\right)\hat{u}(1) = 0.$$

We can now truncate the series to a sum with L unknown coefficients $\hat{a}_\ell$, $l = 0,\dots,L-1$ and match moments, i.e. compare coefficients in the series expansion, to obtain a recurrence relation for $\hat{a}_\ell$, $l = 0,\dots,L-1$,

$$\frac{\kappa^2+s_0^2}{2s_0}\hat{a}_0 + \frac{\kappa^2-s_0^2}{2s_0}\hat{u}(1) = \partial_\nu\hat{u}(1), \qquad (z^0) \tag{3.7}$$

$$\frac{\kappa^2+s_0^2}{2s_0}\hat{a}_1 + 2\frac{\kappa^2-s_0^2}{2s_0}\hat{a}_0 + \frac{\kappa^2+s_0^2}{2s_0}\hat{u}(1) = 0, \qquad (z^1) \tag{3.8}$$

$$\frac{\kappa^2+s_0^2}{2s_0}\hat{a}_{\ell+1} + 2\frac{\kappa^2-s_0^2}{2s_0}\hat{a}_\ell + \frac{\kappa^2+s_0^2}{2s_0}\hat{a}_{\ell-1} = 0, \qquad (z^\ell) \tag{3.9}$$

$$2\frac{\kappa^2-s_0^2}{2s_0}\hat{a}_{L-1} + \frac{\kappa^2+s_0^2}{2s_0}\hat{a}_{L-2} = 0, \qquad (z^L) \tag{3.10}$$

where (3.9) holds for $\ell = 1,\dots,L-2$. This recurrence relation can be very conveniently implemented without an explicit expansion in eigenfunctions (2.3)[2], using a Cartesian product grid structure extending the boundary discretization of the problem. Using finite differences the expansion coefficients can be stored like the unknowns in the interior, see Figure 3.2. In a finite element framework one forms a product with the boundary finite element space taking the expansion coefficients as additional degrees of freedom.

REMARK 3.1. *The equations (3.7)-(3.10) and the system of equations one obtains using a Galerkin ansatz in the Hardy space $H^2(D)$ with a monomial basis, as in [32], are the same, except for (3.10)*[3].

4. Analysis of the Pole Condition Truncation. We first give a reinterpretation of the recurrence relation (3.7)-(3.10) obtained from the PCT as a continued fraction expansion. This interpretation allows us to show that the PCT is a certain Padé approximation of the square root, and to prove a rigorous error estimate for the PCT for our model problem. We then derive an optimal choice of the expansion point s_0 by solving a best approximation problem, and finally also give an interpretation of the recurrence relation (3.7)-(3.10) as a PML.

[2]Multiplications by eigenvalues κ^2 appearing in equations (3.7)-(3.10) are replaced by applications of the discretization of the operator $\partial_{yy} + k^2$.

[3]The $i\kappa_0$ in [32] is our s_0.

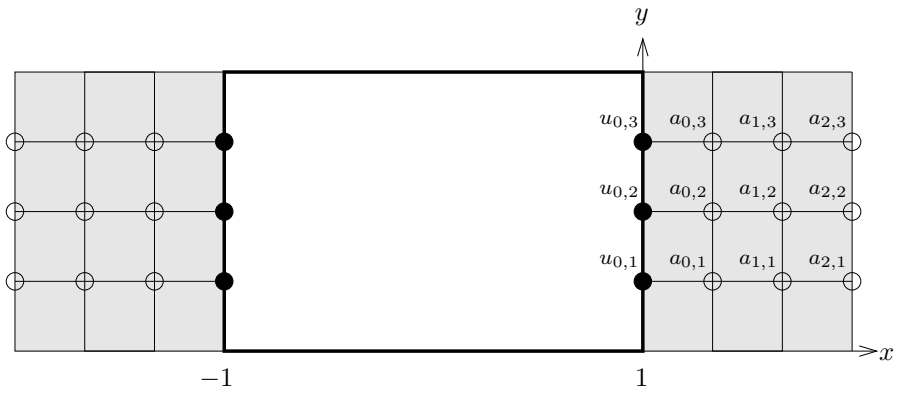

FIG. 3.2. *Implementation of the expansion coefficients on a tensor product grid. In a finite element setting one forms a tensor product of the boundary degrees of freedom with an equidistant grid in x direction. In a finite difference setting the expansion coefficients are treated like a grid function, the same way as the interior unknowns.*

4.1. Interpretation as a continued fraction. Given two sequences of coefficients $(b_\ell)_\ell$ and $(c_\ell)_\ell$, $\ell = 1, 2, \ldots$, the continued fraction is

$$\cfrac{b_1}{c_1 + \cfrac{b_2}{c_2 + \cfrac{b_3}{c_3 + \ldots}}} \quad \text{or in more compact form} \quad \sum_{\ell=1}^{\infty} \frac{b_\ell}{c_\ell +}.$$

Commonly $(b_\ell)_\ell$ is called the numerator sequence and $(c_\ell)_\ell$ the denominator sequence. Following the definition in [31] we introduce for $\ell = 1, 2, \ldots$ the Rotation-Inversion-Translation transform

$$t_\ell : \mathbb{C} \to \mathbb{C} \ , \ x \mapsto \frac{b_\ell}{c_\ell + x},$$

which conveniently allows us to define the L-th approximant of the above continued fraction as composition of t_ℓ, $\ell = 1, \ldots, L$,

$$\sum_{\ell=1}^{L} \frac{b_\ell}{c_\ell +} := t_1 \circ t_2 \circ \cdots \circ t_L(0).$$

In what follows it will be useful to consider improper continued fractions where we "add" the translation $t_0 : x \mapsto c_0 + x$ and obtain

$$c_0 + \sum_{\ell=1}^{L} \frac{b_\ell}{c_\ell +} = t_0 \circ t_1 \circ t_2 \circ \cdots \circ t_L(0).$$

The following theorem, which can be found for example in [28, 31], will be used frequently in what follows.

THEOREM 4.1. *The L-th truncated continued fraction expansion can be repre-*

sented by

$$c_0 + \sum_{\ell=1}^{L} \frac{b_\ell}{c_{\ell+}} = \frac{A_L}{B_L}, \tag{4.1}$$

where A_ℓ and B_ℓ are defined by the recurrence relations

$$\begin{aligned} &A_{-1} = 1, \quad A_0 = c_0, \qquad A_{\ell+1} = c_{\ell+1}A_\ell + b_{\ell+1}A_{\ell-1}, \quad \ell \geq 0, \\ &B_{-1} = 0, \quad B_0 = 1, \qquad B_{\ell+1} = c_{\ell+1}B_\ell + b_{\ell+1}B_{\ell-1}, \quad \ell \geq 0. \end{aligned} \tag{4.2}$$

Proof. See Theorem 6.1 in [28]. ∎

To rewrite the recurrence relations (3.7) - (3.10) as a truncated continued fraction, it is convenient to define the common term appearing to be

$$\alpha := \frac{\kappa^2 - s_0^2}{\kappa^2 + s_0^2}. \tag{4.3}$$

Later, we will also write $\alpha(\kappa^2)$ and view α as a function of κ^2. From the last equation (3.10) of the truncated recurrence relation, we then obtain

$$\hat{a}_{L-1} = \frac{-1}{2\alpha}\hat{a}_{L-2}.$$

Using (3.9) for $\ell = L-2$, which states that $\hat{a}_{L-1} + 2\alpha\hat{a}_{L-2} + \hat{a}_{L-3} = 0$, we get

$$\hat{a}_{L-2} = \frac{-1}{2\alpha + \frac{-1}{2\alpha}}\hat{a}_{L-3} = -\frac{-1}{2\alpha+}\frac{-1}{2\alpha}\hat{a}_{L-3}.$$

Continuing this way we obtain, setting $\ell = 1$ in (3.9),

$$\hat{a}_1 = \left(\sum_{\ell=1}^{L-1} \frac{-1}{2\alpha+}\right)\hat{a}_0.$$

Using the second equation (3.8) of the truncated recurrence equation, which states that $\hat{a}_1 + 2\alpha\hat{a}_0 + \hat{u}(1) = 0$, and the first equation (3.7), we finally get

$$\hat{a}_0 = \left(\sum_{\ell=1}^{L} \frac{-1}{2\alpha+}\right)\hat{u}(1) \quad \text{and} \quad \left(\alpha + \sum_{\ell=1}^{L} \frac{-1}{2\alpha+}\right)\hat{u}(1) = \frac{2s_0}{\kappa^2 + s_0^2}\partial_\nu\hat{u}(1). \tag{4.4}$$

The solution of the truncated recurrence relation (3.7) - (3.10) we obtained for the coefficients can thus be interpreted as an approximation of the DtN map of the form

$$\partial_\nu\hat{u}(1) = \frac{\kappa^2 + s_0^2}{2s_0}\left(\alpha + \sum_{\ell=1}^{L} \frac{-1}{2\alpha+}\right)\hat{u}(1) =: \hat{P}_L(\kappa^2)\hat{u}(1). \tag{4.5}$$

REMARK 4.1. *Using the eigenfunction expansion (2.3) we define, analogously to (2.11), with α_n given by (4.3), where κ^2 is replaced by κ_n^2*

$$P_L u(\pm 1, y) := \sum_n \frac{\kappa_n^2 + s_0^2}{2s_0}\left(\alpha_n + \sum_{\ell=1}^{L} \frac{-1}{2\alpha_n+}\right)\int_0^\pi u(\pm 1, \vartheta)\overline{\psi_n}(\vartheta)d\vartheta\,\psi_n(y), \tag{4.6}$$

which is the PCT expressed as boundary condition.

The following theorem shows that the approximation obtained using the PCT is a truncated continued fraction approximation to the square root appearing in the symbol $i\lambda$ defined in (2.4) of the DtN operator.

THEOREM 4.2. *The PCT defined by the recurrence relations (3.7) - (3.10) converges to the square root representing the symbol $i\lambda_n$ of the DtN operator: with α defined in (4.3) we obtain for $i\lambda_n$ defined in (2.4)*

$$\frac{\kappa^2+s_0^2}{2s_0}\left(\alpha+\sum_{\ell=1}^{\infty}\frac{-1}{2\alpha+}\right)=i\lambda\equiv\begin{cases}-\sqrt{-\kappa^2} & \kappa^2\le 0,\\ i\sqrt{\kappa^2} & \kappa^2>0,\end{cases} \tag{4.7}$$

provided s_0 lies in the fourth quadrant of the complex plane.

Proof. The convergence analysis given here closely follows [31, Sec. 12.3]. First we proof that $\sum_{\ell=1}^{\infty}\frac{-1}{2\alpha+}=-\alpha+\sqrt{\alpha^2-1}$: the recurrence relations satisfied by the numerator and denominator sequences (4.2) are

$$A_{\ell+1}=2\alpha A_\ell-A_{\ell-1}\,,\quad B_{\ell+1}=2\alpha B_\ell-B_{\ell-1},\quad \ell\ge 0. \tag{4.8}$$

The characteristic equation of these recurrence relations is $X^2-2\alpha X+1=0$ with roots

$$\xi_1=\alpha-\sqrt{\alpha-1}\sqrt{\alpha+1}\quad\text{and}\quad \xi_2=\alpha+\sqrt{\alpha-1}\sqrt{\alpha+1} \tag{4.9}$$

such that $\xi_1\xi_2=1$ and $\xi_1+\xi_2=2\alpha$. The function $\alpha:\kappa^2\mapsto\alpha(\kappa^2)$ defined in (4.3) is a Möbius transform, which is sharply 3-transitive, i.e. for any two ordered triples of distinct points, there is a unique transform that maps one triple to the other, mapping generalized circles in the extended complex plane to generalized circles. Hence for $\kappa^2\in\mathbb{R}$, $\alpha(\kappa^2)$ lies on a circle passing through $-1=\alpha(0)$ and $1=\alpha(\infty)$, which can not degenerate to the real axis, since from $\alpha(s_0^2)=0$ it would follow that $s_0^2\in\mathbb{R}$, which contradicts $\Im(s_0)<0$. Hence we have $|\xi_1|<|\xi_2|$. As the two roots are distinct the general solution of (4.8) is $C_1\xi_1^\ell+C_2\xi_2^\ell$, where the constants C_1 and C_2 are determined by the initial conditions $A_{-1}=1, A_0=0, B_{-1}=0, B_0=1$, giving

$$A_\ell=\frac{1}{\xi_1-\xi_2}\left(\xi_1\xi_2^{\ell+1}-\xi_2\xi_1^{\ell+1}\right)\,,\quad B_\ell=\frac{1}{\xi_1-\xi_2}\left(\xi_1^{\ell+1}-\xi_2^{\ell+1}\right).$$

Therefore the L-th approximant is

$$\frac{A_L}{B_L}=-\xi_1\xi_2\frac{\xi_1^L-\xi_2^L}{\xi_1^{L+1}-\xi_2^{L+1}}=-\frac{\xi_2\left(\frac{\xi_1}{\xi_2}\right)^{L+1}-\xi_1}{\left(\frac{\xi_1}{\xi_2}\right)^{L+1}-1}$$

which converges. We obtain

$$\sum_{\ell=1}^{\infty}\frac{-1}{2\alpha+}=\lim_{L\to\infty}\frac{A_L}{B_L}=-\xi_1.$$

Inserting the expression obtained for the continued fraction, we get

$$\begin{aligned}\frac{\kappa^2+s_0^2}{2s_0}(\alpha-\xi_1) &= \frac{\kappa^2+s_0^2}{2s_0}(\alpha-(\alpha-\sqrt{\alpha-1}\sqrt{\alpha+1})\\ &= \frac{\kappa^2+s_0^2}{2s_0}\left(\frac{\kappa^2-s_0^2}{\kappa^2+s_0^2}-1\right)^{\frac{1}{2}}\left(\frac{\kappa^2-s_0^2}{\kappa^2+s_0^2}+1\right)^{\frac{1}{2}}\\ &= \frac{\kappa^2+s_0^2}{2s_0}\left(\frac{-2s_0^2}{\kappa^2+s_0^2}\right)^{\frac{1}{2}}\left(\frac{2\kappa^2}{\kappa^2+s_0^2}\right)^{\frac{1}{2}} = \begin{cases} i\sqrt{\kappa^2} & \text{for } \kappa^2>0\\ -\sqrt{-\kappa^2} & \text{for } \kappa^2\le 0\end{cases},\end{aligned} \tag{4.10}$$

where we used $\sqrt{-1}=i$. ∎

There is a strong connection between Padé approximants and truncated continued fractions, which is used in the following theorem.

THEOREM 4.3. *The pole condition truncation $\hat{P}_L(\kappa^2)$ defined in (4.5), given by the recurrence relation (3.7) - (3.10) up to level L, is a Padé approximation of order $(L+1,L)$ around the expansion point $\kappa^2=-s_0^2$.*

Proof. Let $R_{2L+1}(z)$ be the Padé approximation of order $(L+1,L)$ of $\sqrt{1+z}$ around $z=0$. Below we show that

$$\hat{P}_L(\kappa^2) = -s_0 R_{2L+1}(z) \quad \text{for } z := -\tfrac{s_0^2+\kappa^2}{s_0^2} \in \mathbb{C}. \tag{4.11}$$

A Padé approximation of order $(L+1,L)$ of the binomial function $(1+z)^\nu$ expanded at $z=0$ is given by the truncated continued fraction

$$(1+z)^\nu \approx 1+\cfrac{\nu z}{1\ +}\ \cfrac{(1-\nu)z}{2\ +}\ \cfrac{(1+\nu)z}{3\ +}\ \cfrac{(2-\nu)z}{2\ +}\ \cdots\ \cfrac{(L-\nu)z}{2\ +}\ \cfrac{(L+\nu)z}{2L+1}$$

cf. [5, Page 139, (6.4)], i.e $c_0=1$, $c_{2n-1}=2n-1$, $c_{2n}=2$ for $n=1,\dots$ and $b_{2n+1}=n+\nu$, $b_{2n+2}=n+1-\nu$ for $n=0,\dots$. Setting $\nu=\frac{1}{2}$, a common $(2\ell+1)$ factor cancels, since

$$\cfrac{(\ell+\nu)z}{2\ell+1+\cfrac{(\ell+1-\nu)z}{2}} = \cfrac{(2\ell+1)/2z}{(2\ell+1)+\cfrac{(2\ell+1)/2z}{2}} = \cfrac{\frac{1}{2}z}{1+\cfrac{\frac{1}{2}z}{2}} = \cfrac{z}{2+\frac{z}{2}}.$$

Thus we obtain for the square-root, $\nu=\frac{1}{2}$, that the $(L+1,L)$ Padé approximation can be written as the continued fraction

$$R_{2L+1}(z) := 1+\sum_{\ell=1}^{2L+1}\cfrac{z}{2+}. \tag{4.12}$$

The numerator and denominator sequence for the continued fraction expansion of the Padé approximation to the square root (4.12) are $c_0=1$ and $c_\ell=2$ and $b_\ell=z$ for $\ell\ge 1$. With these R_{2L+1} is given by $\frac{A_{2L+1}}{B_{2L+1}}$ as defined in Theorem 4.1. To obtain recurrence relations for the odd A_ℓ and B_ℓ only we write

$$\begin{array}{rcl|rcl} A_{2\ell+1} &=& 2A_{2\ell}+zA_{2\ell-1}, & B_{2\ell+1} &=& 2B_{2\ell}+zB_{2\ell-1},\\ 2A_{2\ell} &=& 4A_{2\ell-1}+2zA_{2\ell-2}, & 2B_{2\ell} &=& 4B_{2\ell-1}+2zB_{2\ell-2},\\ zA_{2\ell-1} &=& 2zA_{2\ell-2}+z^2A_{2\ell-3}, & zB_{2\ell-1} &=& 2zB_{2\ell-3}+z^2B_{2\ell-3}, \end{array} \tag{4.13}$$

where we multiplied the recurrence relation for $2\ell-1$ by z and the one for 2ℓ by 2. Adding the first two equations and subtracting the last one gives a recurrence relation over a double step,

$$A_{2\ell+1} = 2(2+z)A_{2\ell-1} - z^2 A_{2\ell-3}, \quad B_{2\ell+1} = 2(2+z)B_{2\ell-1} - z^2 B_{2\ell-3}. \tag{4.14}$$

Setting $C_\ell = A_{2\ell-1}$ and $D_\ell = B_{2\ell-1}$ one obtains

$$C_{\ell+1} = 2(2+z)C_\ell - z^2 C_{\ell-1}, \quad D_{\ell+1} = 2(2+z)D_\ell - z^2 D_{\ell-1}, \tag{4.15}$$

with the initial values

$$C_{-1} = 1,\ C_0 = 2+z, \quad D_{-1} = 0,\ D_0 = 2.$$

The solutions of the recurrence relations (4.15) are given by

$$C_\ell = \gamma_1 \mu_1^\ell + \gamma_2 \mu_2^\ell, \quad D_\ell = \delta_1 \mu_1^\ell + \delta_2 \mu_2^\ell,$$

with

$$\mu_{1,2} = z+2 \pm 2\sqrt{z+1}, \quad \gamma_{1,2} = \frac{z+2 \pm 2\sqrt{z+1}}{2}, \quad \delta_{1,2} = \frac{2\sqrt{z+1} \pm (z+2)}{2\sqrt{z+1}},$$

and we thus obtain

$$R_{2L+1}(z) = \frac{C_L}{D_L}. \tag{4.16}$$

The PCT in (4.5) shows that

$$\hat{P}_L(\kappa^2) = s_0 \left(\frac{\kappa^2+s_0^2}{2s_0^2} \frac{\kappa^2-s_0^2}{\kappa^2+s_0^2} - \frac{\frac{\kappa^2+s_0^2}{2s_0^2}}{2\frac{\kappa^2-s_0^2}{\kappa^2+s_0^2} + \frac{-1}{2\alpha+\ldots}} \right),$$

and therefore the numerator and denominator sequences for the continued fraction in the brackets above are

$$\begin{array}{rclcrcll} c_0 &=& \frac{\kappa^2-s_0^2}{2s_0^2}, & & c_\ell &=& 2\frac{\kappa^2-s_0^2}{\kappa^2+s_0^2}, & \text{for } \ell \geq 1, \\ b_1 &=& -\frac{\kappa^2+s_0^2}{2s_0^2}, & & b_\ell &=& -1, & \text{for } \ell \geq 2. \end{array}$$

Setting $z := -\frac{\kappa^2+s_0^2}{s_0^2}$, we obtain $c_0 = -\frac{z+2}{2}$, $c_\ell = (2+z)\frac{2}{z}$ for $\ell = 1, \ldots$, $b_1 = \frac{z}{2}$, and thus get for the numerator $\tilde{C}_L$ and denominator $\tilde{D}_L$ of the rational approximation defined by the recurrence relation (4.2), where $\tilde{C}_L$ plays the role of A_L and $\tilde{D}_L$ the role of B_L,

$$\begin{array}{lll} \tilde{C}_0 = -\frac{z+2}{2}, & \tilde{C}_1 = \frac{z^2+8z+8}{-2z}, & \tilde{C}_{\ell+1} = (2+z)\frac{2}{z}\tilde{C}_\ell - \tilde{C}_{\ell-1}, \quad \ell \geq 1, \\ \tilde{D}_0 = 1, & \tilde{D}_1 = \frac{4+2z}{z}, & \tilde{D}_{\ell+1} = (2+z)\frac{2}{z}\tilde{D}_\ell - \tilde{D}_{\ell-1}, \quad \ell \geq 1, \end{array} \tag{4.17}$$

where instead of $\tilde{C}_{-1}$ and $\tilde{D}_{-1}$ we give explicitly $\tilde{C}_1$ and $\tilde{D}_1$ because b_1 is different from b_ℓ for $\ell \geq 2$. The solution of the recurrence relation (4.17) is given by

$$\tilde{C}_\ell = \hat{\gamma}_1 \hat{\mu}_1^\ell + \hat{\gamma}_2 \hat{\mu}_2^\ell, \quad \tilde{D}_\ell = \hat{\delta}_1 \hat{\mu}_1^\ell + \hat{\delta}_2 \hat{\mu}_2^\ell,$$

with

$$\hat{\mu}_{1,2} = \frac{z+2\pm 2\sqrt{z+1}}{z}, \quad \hat{\gamma}_{1,2} = \frac{z+2\pm 2\sqrt{z+1}}{-4}, \quad \hat{\delta}_{1,2} = \frac{2\sqrt{z+1}\pm(z+2)}{4\sqrt{z+1}}.$$

Comparing with the solution of the recurrence relation (4.15), we see that the extra factor z in the denominator of $\hat{\mu}_{1,2}$ and the extra factor 2 in the denominator of $\hat{\gamma}_{1,2}$ and $\hat{\delta}_{1,2}$ cancel when we take ratios, and thus

$$\frac{\tilde{C}_\ell}{\tilde{D}_\ell} = -\frac{C_\ell}{D_\ell}, \quad \ell \geq 0,$$

which implies that $\hat{P}_L(\kappa^2) = s_0 \frac{\tilde{C}_L}{\tilde{D}_L} = -s_0 \frac{C_L}{D_L} = -s_0 R_{2L+1}(z)$. ∎

We now know that the pole condition provides a Padé approximation of the Dirichlet to Neumann operator. In order to obtain a rigorous error estimate, we will need the following lemma.

LEMMA 4.4. *For all $L \in \mathbb{N}$, the $(L+1, L)$ Padé approximation $R_{2L+1}(z)$ defined in (4.12), satisfies the recurrence relation*

$$R_{\ell+1}(z) = 1 + \frac{z}{1+R_\ell(z)}, \quad \ell = 0, 1, \ldots, 2L, \quad R_0(z) = 1.$$

Proof. We obtain, using (4.12),

$$R_{\ell+1}(z) = 1 + \sum_{j=1}^{\ell+1} \frac{z}{2+} = 1 + \frac{z}{2+\sum_{j=1}^{\ell} \frac{z}{2+}} = 1 + \frac{z}{2+(R_\ell(z)-1)} = 1 + \frac{z}{1+R_\ell(z)}.$$

∎

The next lemma provides the key formula to prove exponential convergence of the PCT, and to optimize the parameter s_0.

LEMMA 4.5. *Let ξ be any root $X^2 - (1+z) = 0$. Then for R_ℓ defined in (4.12) we have for all $\ell = 0, 1, 2, \ldots$ the identity*

$$\frac{\xi + R_\ell(z)}{\xi - R_\ell(z)} = (-1)^\ell \left(\frac{\xi+1}{\xi-1}\right)^{\ell+1}. \tag{4.18}$$

Proof. The proof is by induction: the identity (4.18) holds for $\ell = 0$. So we assume that (4.18) holds for ℓ, and prove that then (4.18) also holds for $\ell+1$, by computing

$$\frac{\xi + R_{\ell+1}(z)}{\xi - R_{\ell+1}(z)} = \frac{\xi + (1 + \frac{z}{1+R_\ell(z)})}{\xi - (1 + \frac{z}{1+R_\ell(z)})} = \frac{\xi(1+R_\ell(z)) + (R_\ell(z)+\xi^2)}{\xi(1+R_\ell(z)) - (R_\ell(z)+\xi^2)}$$

$$= \frac{\xi + \xi R_\ell(z) + R_\ell(z) + \xi^2}{\xi + \xi R_\ell(z) - R_\ell(z) - \xi^2} = -\frac{\xi+1}{\xi-1}\frac{\xi + R_\ell(z)}{\xi - R_\ell(z)} = (-1)^{\ell+1}\left(\frac{\xi+1}{\xi-1}\right)^{\ell+2}.$$

REMARK 4.2. *In terms of κ^2, using that $z = -\frac{s_0^2+\kappa^2}{s_0^2}$ as defined in (4.11), the expression in the parentheses on the right in (4.18) is*

$$\frac{\xi+1}{\xi-1} = \frac{\chi + s_0}{\chi - s_0},$$

where ξ is any root of $X^2-(1+z)=0$ and χ is any root of $X^2+\kappa^2=0$. Thus we obtain from (4.18) for $\ell = 2L+1$, and using the relation between the Padé approximation and the PCT in (4.11) that

$$\frac{i\lambda_n - \hat{P}_L(\kappa_n^2)}{i\lambda_n + \hat{P}_L(\kappa_n^2)} = \frac{i\lambda_n + s_0 R_{2L+1}(z)}{i\lambda_n - s_0 R_{2L+1}(z)} = \left(\frac{i\lambda_n + s_0}{i\lambda_n - s_0}\right)^{2(L+1)},$$

where $i\lambda_n$ is the root defined in (2.4), which we will use in the next section to obtain an error estimate.

4.2. Error estimate. Let u be the exact solution of the Helmholtz equation (2.12) on the bounded domain Ω_{int} with the exact DtN map defined in (2.11), and let $\tilde{u}$ be the solution obtained using the PCT (4.6) to truncate the computational domain,

$$\begin{aligned} -(\partial_{xx}+\partial_{yy}+k^2)\tilde{u} &= f && \text{in } \Omega_{int}, \\ \tilde{u} &= 0 && \text{on } [-1,1]\times\{0,\pi\}, \\ \partial_\nu \tilde{u} &= P_L\tilde{u} && \text{on } \{-1,1\}\times(0,\pi). \end{aligned} \tag{4.19}$$

As $\partial_\nu u - \mathrm{DtN}u = 0$ for $x=\pm 1$, we obtain for the error $e := u-\tilde{u}$

$$\begin{aligned} -(\partial_{xx}+\partial_{yy}+k^2)e &= 0 && \text{in } \Omega_{int}, \\ e &= 0 && \text{on } [-1,1]\times\{0,\pi\}, \\ (\partial_\nu - P_L)e &= (\mathrm{DtN}-P_L)u && \text{on } \{\pm 1\}\times(0,\pi). \end{aligned} \tag{4.20}$$

Using a decomposition of e in terms of eigenmodes of the boundary operator, the general solution of (4.20) is

$$\hat{e}_n = C_{1,n}\mathrm{e}^{i\lambda_n x} + C_{2,n}\mathrm{e}^{-i\lambda_n x}.$$

Note that λ_n is a function of κ_n via (2.4). We define $\phi_n^+(x) := \mathrm{e}^{i\lambda_n x}$ and $\phi_n^-(x) := \mathrm{e}^{-i\lambda_n x}$. In what follows we write $\hat{P}_L$ instead of $\hat{P}_L(\kappa_n^2)$. At the right boundary, $x=1$, where $\partial_\nu = \partial_x$, by the definition of the DtN given in (2.11) and the last equation in (4.20), we get

$$\begin{aligned} (\partial_\nu - \hat{P}_L)\hat{e}_n|_{x=1} &= (i\lambda_n - \hat{P}_L)C_{1,n}\mathrm{e}^{i\lambda_n} - (i\lambda_n + \hat{P}_L)C_{2,n}\mathrm{e}^{-i\lambda_n} \\ &= (i\lambda_n - \hat{P}_L)\hat{u}_n|_{x=1}. \end{aligned}$$

A similar calculation at the left boundary, where $\partial_\nu = -\partial_x$, shows that

$$\begin{aligned} (\partial_\nu - \hat{P}_L)\hat{e}_n|_{x=-1} &= -(i\lambda_n + \hat{P}_L)C_{1,n}\mathrm{e}^{-i\lambda_n} + (i\lambda_n - \hat{P}_L)C_{2,n}\mathrm{e}^{i\lambda_n} \\ &= (i\lambda_n - \hat{P}_L)\hat{u}_n|_{x=-1}. \end{aligned}$$

From these one obtains $C_{1,n}$ and $C_{2,n}$ from the linear system

$$\begin{bmatrix} (i\lambda_n - \hat{P}_L)\mathrm{e}^{i\lambda_n} & -(i\lambda_n + \hat{P}_L)\mathrm{e}^{-i\lambda_n} \\ -(i\lambda_n + \hat{P}_L)\mathrm{e}^{-i\lambda_n} & (i\lambda_n - \hat{P}_L)\mathrm{e}^{i\lambda_n} \end{bmatrix} \begin{bmatrix} C_{1,n} \\ C_{2,n} \end{bmatrix} = \begin{bmatrix} (i\lambda_n - \hat{P}_L)\hat{u}_n(1) \\ (i\lambda_n - \hat{P}_L)\hat{u}_n(-1) \end{bmatrix}. \tag{4.21}$$

Let $d_n := ((i\lambda_n - \hat{P}_L)\phi_n^+(1))^2 - ((i\lambda_n + \hat{P}_L)\phi_n^-(1))^2$ be the determinant of the matrix in (4.21), and

$$\tilde{\rho}_n := \frac{i\lambda_n - \hat{P}_L}{i\lambda_n + \hat{P}_L}. \tag{4.22}$$

Then the error is given by

$$\hat{e}_n(x) = \begin{bmatrix}\phi_n^+(x)\\ \phi_n^-(x)\end{bmatrix}^T \begin{bmatrix}C_{1,n}\\ C_{2,n}\end{bmatrix} \tag{4.23a}$$

$$= \frac{i\lambda_n - \hat{P}_L}{d_n} \begin{bmatrix}(i\lambda_n - \hat{P}_L)\phi_n^+(x+1) + (i\lambda_n + \hat{P}_L)\phi_n^-(x+1)\\ (i\lambda_n + \hat{P}_L)\phi_n^+(x-1) + (i\lambda_n - \hat{P}_L)\phi_n^-(x-1)\end{bmatrix}^T \begin{bmatrix}\hat{u}_n(1)\\ \hat{u}_n(-1)\end{bmatrix} \tag{4.23b}$$

$$= \frac{i\lambda_n - \hat{P}_L}{i\lambda_n + \hat{P}_L} \begin{bmatrix}\frac{\frac{i\lambda_n-\hat{P}_L}{i\lambda_n+\hat{P}_L}\phi_n^+(x+1)+\phi_n^-(x+1)}{\left(\frac{i\lambda_n-\hat{P}_L}{i\lambda_n+\hat{P}_L}\phi_n^+(1)\right)^2-\phi_n^-(1)^2}\\ \frac{\frac{i\lambda_n-\hat{P}_L}{i\lambda_n+\hat{P}_L}\phi_n^-(x-1)+\phi_n^+(x-1)}{\left(\frac{i\lambda_n-\hat{P}_L}{i\lambda_n+\hat{P}_L}\phi_n^+(1)\right)^2-\phi_n^-(1)^2}\end{bmatrix}^T \begin{bmatrix}\hat{u}_n(1)\\ \hat{u}_n(-1)\end{bmatrix} \tag{4.23c}$$

$$= \tilde{\rho}_n \begin{bmatrix}\frac{\tilde{\rho}_n\phi_n^+(x+1)+\phi_n^-(x+1)}{\left(\tilde{\rho}_n\phi_n^+(1)\right)^2-\phi_n^-(1)^2}\\ \frac{\tilde{\rho}_n\phi_n^-(x-1)+\phi_n^+(x-1)}{\left(\tilde{\rho}_n\phi_n^+(1)\right)^2-\phi_n^-(1)^2}\end{bmatrix}^T \begin{bmatrix}\hat{u}_n(1)\\ \hat{u}_n(-1)\end{bmatrix} \tag{4.23d}$$

$$= \tilde{\rho}_n \mathrm{e}^{2i\lambda_n} \begin{bmatrix}\frac{\tilde{\rho}_n\phi_n^+(x+1)+\phi_n^-(x+1)}{(\tilde{\rho}_n\mathrm{e}^{2i\lambda_n})^2-1}\\ \frac{\tilde{\rho}_n\phi_n^-(x-1)+\phi_n^+(x-1)}{(\tilde{\rho}_n\mathrm{e}^{2i\lambda_n})^2-1}\end{bmatrix}^T \begin{bmatrix}\hat{u}_n(1)\\ \hat{u}_n(-1)\end{bmatrix}. \tag{4.23e}$$

Now by the Cauchy Schwarz inequality we can bound $|e_n(x)|$ in terms of the Dirichlet data. Using then Parseval's theorem we obtain

$$\begin{aligned}\|e(x,\cdot)\|_2^2 = \sum_n |\hat{e}_n(x)|^2 &\le \sum_n 2\chi(\lambda_n,x)^2(|\hat{u}_n(1)|^2 + |\hat{u}_n(-1)|^2)\\ &\le 2\sup_n \chi(\lambda_n,x)^2(\|u(1,\cdot)\|_2^2 + \|u(-1,\cdot)\|_2^2),\end{aligned}$$

where $\chi(\lambda_n, x)$ is given, using (4.23e), as

$$\chi(\lambda_n,x)^2 := |\tilde{\rho}_n|^2 \frac{|\tilde{\rho}_n\mathrm{e}^{i\lambda_n(x+3)} + \mathrm{e}^{i\lambda_n(1-x)}|^2 + |\tilde{\rho}_n\mathrm{e}^{(3-x)\lambda_n} + \mathrm{e}^{(x+1)\lambda_n}|^2}{|\,(\tilde{\rho}_n\mathrm{e}^{2i\lambda_n})^2 - 1|^2}. \tag{4.24}$$

We have thus proved the following error estimate:

THEOREM 4.6. *With $\chi(\lambda_n, x)$ defined in (4.24), the error of the solution obtained using the PCT boundary condition is bounded for all $x \in [-1, 1]$ by*

$$\|e(x,\cdot)\|_2^2 \le 2\sup_n \chi(\lambda_n,x)^2(\|u(1,\cdot)\|_2^2 + \|u(-1,\cdot)\|_2^2). \tag{4.25}$$

This estimate shows that in order to obtain a good PCT boundary condition, $\chi(\lambda_n, x)^2$ should be small for all n and all $x \in [-1, 1]$. We will study in the next section how this can be achieved choosing a good expansion point s_0 for the PCT.

4.3. Optimized choice of s_0. From the error estimate in the previous subsection, we can determine the expansion point s_0 such that the error bound becomes as small as possible to obtain good performance of the PCT. If we choose for example the maximum norm in x, this means we would have to solve the min-max problem

$$\min_{s_0} \max_n \Big(\max_{x\in[-1,1]} \chi(\lambda_n, x) \Big). \tag{4.26}$$

We show in Figure 4.1 the numerical solution of this min-max problem for a specific example where we assume that both the real and the imaginary λ lie in the interval

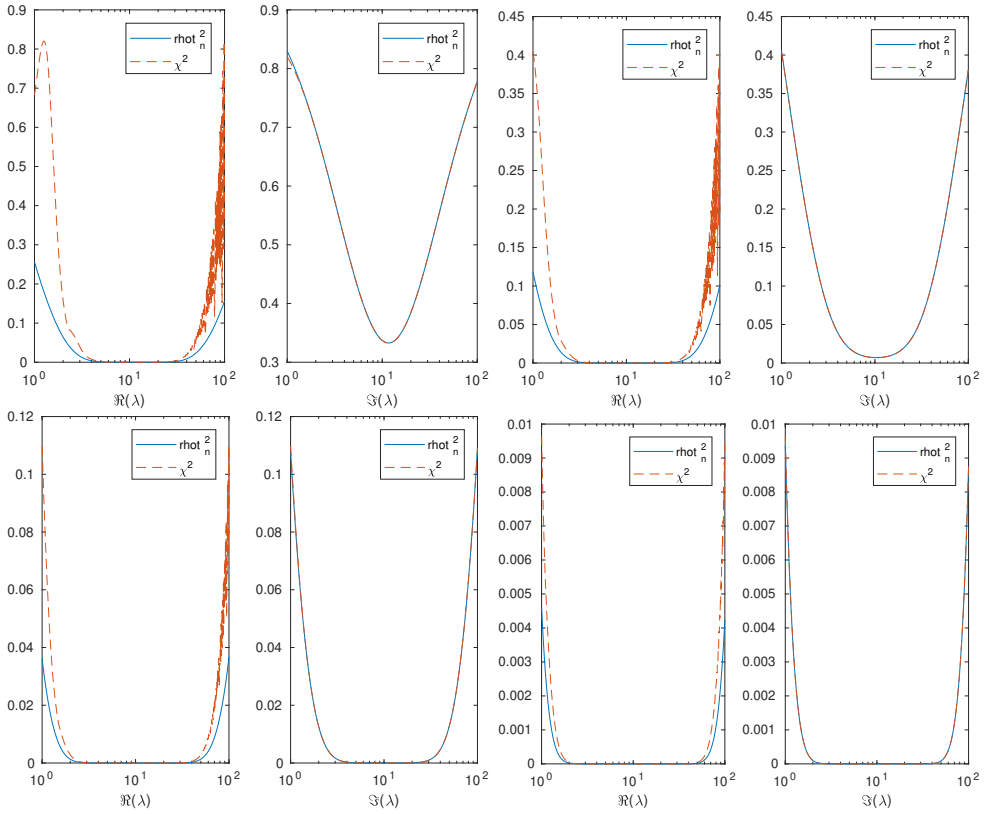

FIG. 4.1. *Numerical solution of the min-max problem* (4.26) *compared to the value of the simpler quantity* $\tilde{\rho}_n$.

[1, 100], and we use a PCT truncation level $L = 1, 2, 4, 8$ from the top left to the bottom right, showing each time the maximum norm $\max_{x\in[-1,1]} \chi(\lambda_n, x)$ for λ_n (real or imaginary in two plots next to each other) at the numerically optimized s_0. We see that increasing L makes the error bound χ^2 shown in red rapidly small for both real and imaginary λ. For real λ, there is a rapid oscillation in χ which indicates that an analytical treatment of this problem is very hard, whereas for imaginary λ this is not the case. These experiments show that at the solution of the min-max problem the error is largest at the boundaries of the intervals, both for real and imaginary λ when L becomes larger. In addition, we see that the solution is characterized by an equioscillation property between the boundaries of the real λ and one boundary of the imaginary λ in this example. But most importantly, for this optimized s_0 also the simpler factor $\tilde{\rho}_n^2$ shows the same equioscillation property as soon as L becomes larger. To determine a good choice of s_0, we thus now study the min-max problem for $\tilde{\rho}_n$,

$$\min_{s_0} \max_n |\tilde{\rho}_n| = \min_{s_0} \max_n \left| \frac{i\lambda_n - \hat{P}_L}{i\lambda_n + \hat{P}_L} \right|, \tag{4.27}$$

which is amenable to analysis using Lemma 4.5, and we will see that equioscillation always holds in three points.

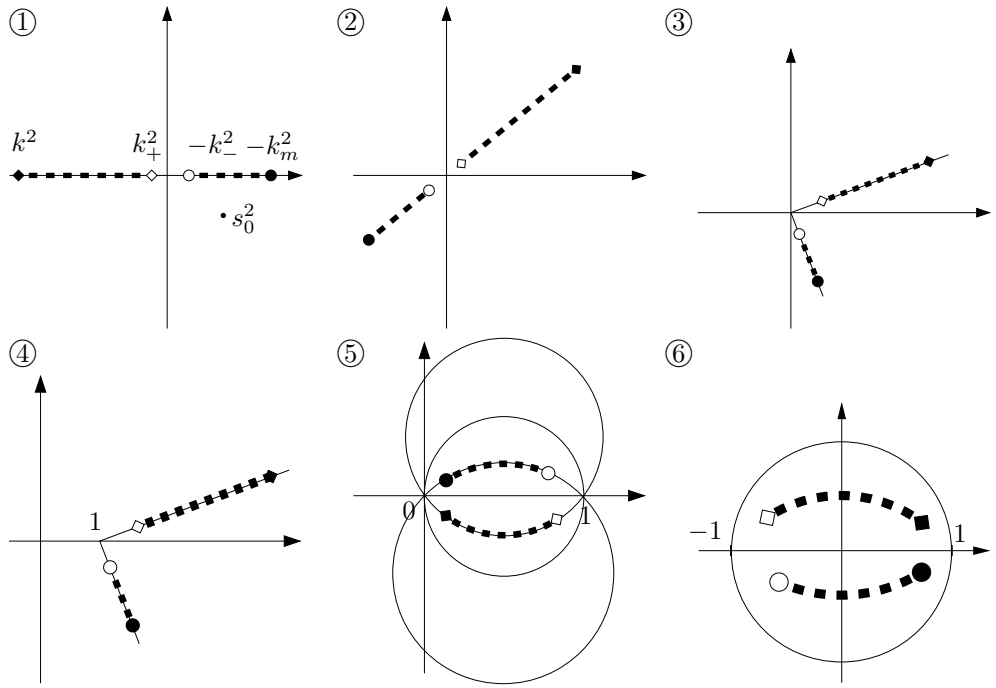

FIG. 4.2. *Cartoon for the mapping of* $[-k_m^2,-k_-^2]\cup[k_+^2,k^2]$ *(dashed lines) in the complex plane by the Möbius transform* $\mathcal{M}:\kappa^2\mapsto\frac{\sqrt{-\kappa^2/s_0^2}-1}{\sqrt{-\kappa^2/s_0^2}+1}=1-\frac{2}{\sqrt{-\kappa^2/s_0^2}+1}$*, which is a composition of a multiplication by* -1 *(1st image), rotation and scaling by* s_0^{-2} *(2nd image), taking the square-root (3rd image), a shift by 1 to the right (4th image), an inversion (5th image), such that* $[-k_m^2,-k_-^2]\cup[k_+^2,k^2]$ *is mapped to two segments on two circles intersecting at* 0 *and* 1 *inside the ball with center and radius* $\frac{1}{2}$*, and a multiplication by* -2 *and a shift by* 1 *(6th image), such that finally* $\mathcal{M}([-k_m^2,-k_-^2]\cup[k_+^2,k^2])$ *is contained inside the unit-disc.*

4.3.1. Rigorous estimate. By our definition of the square root we have $|e^{2i\sqrt{\lambda_n}}|\leq$ 1 which gives, using the variable z instead of λ,

$$|\tilde{\rho}_n(\kappa_n^2)|=\frac{|i\lambda_n(\kappa_n^2)-\hat{P}_L(\kappa_n^2)|}{|i\lambda_n(\kappa_n^2)+\hat{P}_L(\kappa_n^2)|}=\frac{|\sqrt{z-1}-R_{2L-1}(z)|}{|\sqrt{z+1}+R_{2L-1}(z)|}.$$

By Lemma 4.5 and Remark 4.2 it suffices to discuss the mapping $z\mapsto\frac{\sqrt{-z/s_0^2}-1}{\sqrt{-z/s_0^2}+1}$ for $z=\kappa^2$, where in our model problem $\kappa^2\in(-\infty,k^2]\backslash\{0\}$ is an eigenvalue of the operator $(\partial_{yy}+k^2)$. We assume that k^2 and the discretization of ∂_{yy} are such that there are $k_-,k_+\neq 0$ such that $\kappa^2\in[-k_m^2,-k_-^2]\cup[k_+^2,k^2]$, i.e. κ^2 is in bounded intervals and it is bounded away from 0.

As indicated in Figure 4.2 for any $s_0=x_1+ix_2$ in the fourth quadrant, i.e. s_0^2 in the lower complex half plane, the mapping $z\mapsto\frac{\sqrt{-z/s_0^2}-1}{\sqrt{-z/s_0^2}+1}$ maps line segments on the negative real axis and on the positive real axis to two arcs in the unit disc. As the Möbius transform is a conformal mapping these two arcs intersect in ±1 with an angle of 90 degrees.

Hence in order to minimize the modulus of the image of $[-k_m^2,-k_-^2]\cup[k_+^2,k^2]$ it suffices to consider the end points of the line segments. For purely imaginary z,

$z = i\upsilon$ we have

$$\frac{|i\upsilon - (x_1 + ix_2)|}{|i\upsilon + (x_1 + x_2)|} = \frac{\sqrt{x_1^2 + (x_2 - \upsilon)^2}}{\sqrt{x_1^2 + (x_2 + \upsilon)^2}},$$

and for real z, $z = -\upsilon$ we have

$$\frac{|-\upsilon - (x_1 - +ix_2)|}{|-\upsilon + (x_1 + ix_2)|} = \frac{\sqrt{x_2^2 + (x_1 + \upsilon)^2}}{\sqrt{x_2^2 + (x_1 - \upsilon)^2}}.$$

The square of the modulus of the end points of the two arcs are given by

$$r_1(x_1, x_2) = \frac{(k - x_2)^2 + x_1^2}{(k + x_2)^2 + x_1^2}, \quad r_2(x_1, x_2) = \frac{(k_+ - x_2)^2 + x_1^2}{(k_+ + x_2)^2 + x_1^2}$$

and

$$r_3(x_1, x_2) = \frac{(k_- - x_1)^2 + x_2^2}{(k_- + x_1)^2 + x_2^2}, \quad r_4(x_1, x_2) = \frac{(k_m - x_1)^2 + x_2^2}{(k_m + x_1)^2 + x_2^2}.$$

The optimal $s_0 = x_1 + ix_2$ is thus given as the solution of the min-max problem

$$\min_{x_1, x_2 \in \mathbb{R}^+} \max_{j=1,\ldots,4} \{r_j\}.$$

Introducing the auxiliary variable $x_3 = \max_{j=1,\ldots,4}\{r_j\}$, setting $x = (x_1, x_2, x_3)$ and $f_i(x) = r_j(x_1, x_2) - x_3$ for $j = 1, \ldots, 4$, $f_5(x) = -x_1$ and $f_6(x) = -x_2$ this min-max problem is equivalent, cf [37], to the smooth constrained optimization problem

$$\min_{x \in \mathbb{R}^3} x_3 \quad \text{subject to } f_j(x) \le 0, \quad \text{for } j = 1, \ldots, 6. \tag{4.28}$$

For Lagrange multipliers $\eta = (\eta_1, \ldots, \eta_6)$ set $L(x, \eta) = x_3 + \sum_{j=1}^6 \eta_j f_j(x)$. Using Maple we solve $\nabla_x L(x, \eta) = 0$ and the complementary condition $\eta_j f_j(x) = 0$ for $j = 1, \ldots, 6$, from the first order necessary conditions, [35, Satz 9.1.15], and obtain candidates for a solution (x^*, η^*). Assuming that $k, k_+, k_-, k_m > 0$ and additionally that $k > k_+$ and $k_- < k_m$ and requiring that $\eta_j^* \ge 0$ and $f_j(x^*) \ge 0$ for $j = 1, \ldots, 6$, we find only one Karush-Kuhn-Tucker point for (4.28) with $x_3 < 1$ depending on simple relations between k, k_+, k_- and k_m. We obtain six cases:
1. Case: $k > k_m$ and $k_+ > k_-$:

$$x_1 = x_2 = \sqrt{\frac{kk_-}{2}}, x_3 = \frac{k + k_- - \sqrt{2kk_-}}{k + k_- + \sqrt{2kk_-}}.$$

2. Case: $k_m > k$ and $k_- > k_+$:

$$x_1 = x_2 = \sqrt{\frac{k_+k_m}{2}}, x_3 = \frac{k_+ + k_m - \sqrt{2k_+k_m}}{k_+ + k_m + \sqrt{2k_+k_m}}.$$

3. Case: $k > k_m$ and $k_- > k_+$, where we distinguish two subcases:
3a) Subcase: $k_-k_m > kk_+$:

$$x_1 = \frac{\sqrt{kk_+}(kk_+ + k_m^2)}{\sqrt{k_{4,3}}}, x_2 = \frac{\sqrt{kk_+}k_m(k + k_+)}{\sqrt{k_{4,3}}}, x_3 = \frac{-2\sqrt{kk_+k_{4,3}}k_m + k_{4,3}}{2k_m\sqrt{kk_+k_{4,3}} + k_{4,3}},$$

where $k_{4,3} = (k_m^2 + kk_+)^2 + k_m^2(k + k_+)^2$.

3b) Subcase: $kk_+ > k_-k_m$:

$$x_1 = \frac{\sqrt{kk_+}(kk_+ + k_-^2)}{\sqrt{k_{3,4}}}, x_2 = \frac{\sqrt{kk_+}k_-(k+k_+)}{\sqrt{k_{3,4}}}, x_3 = \frac{-2\sqrt{kk_+k_{3,4}}k_- + k_{3,4}}{k_{3,4} + 2k_m\sqrt{kk_+k_{3,4}}},$$

where $k_{3,4} = (k_-^2 + kk_+)^2 + k_-^2(k+k_+)^2$.

4. Case: $k_m > k$ and $k_+ > k_-$, where we again distinguish two subcases:

4a) Subcase: $k_-k_m > kk_+$:

$$x_1 = \frac{\sqrt{k_-k_m}k_+(k_- + k_m)}{\sqrt{k_{2,1}}}, x_2 = \frac{\sqrt{k_-k_m}(k_-k_m + k_+^2)}{\sqrt{k_{2,1}}}, x_3 = \frac{-2\sqrt{k_-k_mk_{2,1}}k_+ + k_{2,1}}{k_{2,1} + 2k_+\sqrt{k_+k_mk_{2,1}}},$$

where $k_{2,1} = (k_+^2 + k_-k_m)^2 + k_+^2(k_- + k_m)^2$.

4b) Subcase: $kk_+ > k_-k_m$:

$$x_1 = \frac{\sqrt{k_-k_m}k(k_- + k_m)}{\sqrt{k_{1,2}}}, x_2 = \frac{\sqrt{k_-k_m}(k_-k_m + k^2)}{\sqrt{k_{1,2}}}, x_3 = \frac{-2\sqrt{k_-k_mk_{1,2}}k + k_{1,2}}{k_{1,2} + 2k\sqrt{k_+k_mk_{1,2}}}.$$

where $k_{1,2} = (k^2 + k_-k_m)^2 + k^2(k_- + k_m)^2$.

In each case (x_1, x_2, x_3) satisfy Robinson's constraint qualification [35]. Checking the second order sufficient conditions [35, Satz 9.2.8], we find that there is a strict local minimum in cases 1 and 2. It was not possible to check the second order sufficient conditions for the four remaining cases. However numerical examples indicate that in cases 3 and 4 we have indeed a global minimum.

Mathematically, it is interesting to have k_m become large, all the other k's remaining fixed, which corresponds to mesh refinement keeping the wavenumber k fixed. This implies that we must be in case 2 or case 4a) above. Assuming that k_m goes to infinity, we get the asymptotic relations

(4.29)

$$\begin{aligned} &k_- > k_+ : \quad x_1 = x_2 \sim \sqrt{\tfrac{k_+}{2}}\sqrt{k_m},\ x_3 \sim 1 - 2^{\frac{3}{2}}\sqrt{k_+}\tfrac{1}{\sqrt{k_m}}, \\ &k_- < k_+ : \quad x_1 \sim \tfrac{\sqrt{k_-k_+}}{\sqrt{k_-^2+k_+^2}}\sqrt{k_m},\ x_2 \sim \tfrac{k_-^{\frac{3}{2}}}{\sqrt{k_-^2+k_+^2}}\sqrt{k_m},\ x_3 \sim 1 - \tfrac{2k_+(\sqrt{k_+}+\sqrt{k_-})}{\sqrt{k_-^2+k_+^2}}\tfrac{1}{\sqrt{k_m}}. \end{aligned}$$

For engineering purposes in practice, one often chooses 10 points per wavelength, which means that $k_m \sim k$, but k_m larger by a multiplicative constant, say $k_m = Ck$ with $C > 1$. Then still case 2 and case 4 apply, but now it could be 4a) or 4b). We still get when k_m becomes large asymptotically the results in (4.29), except when $k_- < k_+$ and $k_+ > k_-C$, case 4b), where

$$x_1 \sim C\sqrt{k_-}\sqrt{k_m},\ x_2 \sim \sqrt{k_-}\sqrt{k_m},\ x_3 \sim 1 - 2C(\sqrt{k_+} + \sqrt{k_-})\frac{1}{\sqrt{k_m}}. \tag{4.30}$$

Finally, to avoid the pollution effect, one would choose k_m growing faster than k, and in this case, we are again asymptotically in case 2 or 4a) with the results given in (4.29). This shows that in all cases, the optimized coordinate choice of the point s_0 behaves like $\sqrt{k_m}$, and the associated error like $1 - O(k_m^{-\frac{1}{2}})$, only the constants are different.

For growing k_m, the error in Theorem 4.6 scales like $(1 - O(k_m^{-\frac{1}{2}}))^{2L}$ for L unknown coefficients. This is not as good as what can be obtained from a best rational

approximation: for large L, the optimal rational approximation f_L on the interval $[k_-, k_m]$ yields

$$\max_{\lambda\in[k_-,k_m]} |f_L(\lambda) - \lambda^{-\frac{1}{2}}| = O(\exp(-\pi^2 L/\log(\tfrac{k_m}{k_-}))).$$

This is Zolotarev's optimal rational approximation for the square root, see e.g. [34]. Using this result it is shown in [26] that the error for the rational best approximation is $O(\exp(-L/\log(k_m)))$.

5. Connection to PML. We would finally like to point out a connection of the PCT to the PML technique. We use the same discrete PML as Gudatti and Lim [21], so their continued fraction approximation is a Padé approximation. As we mentioned already, the recurrence relation obtained by the pole condition can be conveniently implemented extending just the interior grid, see Figure 3.2. We are interested now in giving a direct interpretation of the coefficients stored on the extended grid. Alternatively one could show, that the continued fraction obtained in [21] is equivalent to the PCT.

Equations (3.7) to (3.10) should be interpreted as an approximate DtN operator in the following sense: given the Dirichlet data $u(1, y)$ or its numerical approximation, the solution of the linear system of equations (3.7) to (3.10) for the $L + 1$ unknowns $a_0, \dots, a_{L-1}$, and $\partial_\nu u(1, y)$ defines a mapping $u(1, y) \mapsto \partial_\nu u(1, y)$. If we set $a_{-1} = u(1, y)$ then (3.7) to (3.10) can be rewritten as

$$\frac{s_0^2 + A}{2s_0} a_0 + \frac{-s_0^2 + A}{2s_0} a_{-1} = \partial_\nu u, \tag{5.1}$$

$$\frac{s_0^2 + A}{2s_0} a_{\ell+1} + 2\frac{-s_0^2 + A}{2s_0} a_\ell + \frac{s_0^2 + A}{2s_0} a_{\ell-1} = 0, \quad \text{for } \ell = 0, \dots, L-2, \tag{5.2}$$

$$2\frac{-s_0^2 + A}{2s_0} a_{L-1} + \frac{s_0^2 + A}{2s_0} a_{L-2} = 0, \tag{5.3}$$

where A is the operator $\partial_{yy} + k^2$ or its discretization. For the domain truncation by a PML, the solution in the exterior ($x > 1$ in our case) is analytically continued to the complex plane. There, a path with parameterization γ,

$$\gamma(x) := x + \int_0^x \sigma(\xi) d\xi,$$

is chosen, i.e. $\sigma(\xi) = 0$ for $\xi < 1$. One then defines the complex scaled function $\tilde{u}(x, y) = u(\gamma(x), y)$. The PML layer is truncated at $x = R$ with a homogeneous Dirichlet boundary condition. To use the PML numerically, one choses a mesh with mesh points $1 = x_0 < x_1 < \cdots < x_L = R$ for the interval $(1, R)$, with mesh size $h_\ell := x_\ell - x_{\ell-1}$, and introduces piecewise linear hat functions ψ_ℓ such that $\psi_\ell(x_j) = \delta_{\ell j}$. The space of test functions is $V = \text{span}\{\psi_\ell : \ell = 1, \dots, L-1\} \subset H_0^1((1, R))$ and the trial functions are chosen from $W = a_{-1}\psi_0 + \text{span}\{\psi_\ell : \ell = 1, \dots, L-1\} \subset H^1((0, 1))$. Then $\tilde{u}_R(x, y)$ as a function of x is a solution of the variational formulation: Find $u \in W$ such that

$$\int_1^R -\frac{1}{\gamma'(x)} \partial_x u \frac{1}{\gamma'(x)} \partial_x v \gamma'(x) + Auv\gamma'(x) dx = 0 \quad \forall v \in V_0. \tag{5.4}$$

If we use the midpoint rule for the integration on each finite element, then we obtain

for the unknown coefficient functions u_ℓ, $\ell = 1, \dots L-1$, the linear system of equations

$$\frac{1}{h_\ell \gamma_\ell} u_{\ell-1} - \left(\frac{1}{h_\ell \gamma_\ell} + \frac{1}{h_{\ell+1}\gamma_{\ell+1}} \right) u_\ell + \frac{1}{h_{\ell+1}\gamma_{\ell+1}} u_{\ell+1} +$$

$$A \left(\frac{h_\ell \gamma_\ell}{4} u_{\ell-1} + \frac{h_{\ell+1}\gamma_{\ell+1} + h_\ell \gamma_\ell}{4} u_\ell + \frac{h_{\ell+1}\gamma_{\ell+1}}{4} u_{\ell+1} \right) = 0 \; ; \ell = 1 \dots, L-2 \tag{5.5}$$

$$\frac{1}{h_{L-1}\gamma_{L-1}} u_{L-2} - \left(\frac{1}{h_{L-1}\gamma_{L-1}} + \frac{1}{h_L \gamma_L} \right) u_{L-1} +$$

$$A \left(\frac{h_{L-1}\gamma_{L-1}}{4} u_{L-2} + \frac{h_{L-1}\gamma_{L-1} + h_L \gamma_L}{4} u_{L-1} \right) = 0, \tag{5.6}$$

where $\gamma_j := \gamma'(\frac{x_j + x_{j-1}}{2})$ is the evaluation at the element midpoint and $u_0 = a_{-1}$. If we work with an equidistant grid, $h_\ell = h$, the Neumann data for the exterior domain is recovered by

$$-\frac{1}{h\gamma_0} u_0 + \frac{1}{h\gamma_0} u_1 + hA \left(\frac{\gamma_0}{4} u_0 + \frac{\gamma_0}{4} u_1 \right) = -\frac{1}{\gamma'(1)} \partial_{\nu,ext} \tilde{u}(1, y). \tag{5.7}$$

We have $\frac{1}{\gamma'(1)} \partial_{\nu,ext} \tilde{u}(1,y) = -\partial_\nu u(1,y)$ by the definition of $\tilde{u}$. For the special choice $\gamma_\ell = \frac{2}{h s_0}$, the PCT (5.1)-(5.3) defines the same approximate DtN map as the PML (5.7), (5.5) and (5.6). We have thus proved that a PML with a constant complex stretching $\sigma(x) := \frac{2}{h s_0}$ discretized with P_1 finite elements on an equidistant mesh with mesh size h is equivalent to the PCT, and thus represents a Padé approximation of the symbol of the DtN around the expansion point s_0 chosen in the complex stretching of the PML. For a constant stretching in the PML, we have thus determined the optimal value.

6. Conclusion. We have shown that for the model problem of the Helmholtz equation in an infinite strip, the pole condition, discretized with a matching moment approach gives an absorbing boundary condition of Padé type. This relationship allowed us also to prove that the pole condition truncation is exponentially convergent in this case, and we determined an optimized choice for the expansion point in the pole condition which minimizes our error bound. We finally showed that the matched moments stored naturally on a continuation of the grid can also be interpreted as a perfectly matched layer to truncate the unbounded domain, when a constant complex stretching on an equidistant grid is used. Our results thus provide a direct and natural mathematical relation between absorbing boundary conditions, perfectly matched layers and the pole condition.

REFERENCES

[1] X. Antoine, A. Arnold, C. Besse, M. Ehrhardt, and A. Schädle, *A review of transparent and artificial boundary conditions techniques for linear and nonlinear Schrödinger equations*, Commun. Comput. Phys., 4 (2008), pp. 729–796.

[2] X. Antoine, M. Darbas, and Y. Y. Lu, *An improved surface radiation condition for high-frequency acoustic scattering problems*, Comput. Methods Appl. Mech. Engrg., 195 (2006), pp. 4060–4074.

[3] A. V. Astaneh and M. N. Guddati, *A two-level domain decomposition method with accurate interface conditions for the Helmholtz problem*, International Journal for Numerical Methods in Engineering, 107 (2016), pp. 74–90.

[4] S. Asvadurov, V. Druskin, M. N. Guddati, and L. Knizhnerman, *On optimal finite-difference approximation of PML*, SIAM J. Numer. Anal., 41 (2003), pp. 287–305.

[5] G. A. Baker, Jr. and P. Graves-Morris, *Padé approximants. Part I*, vol. 13 of Encyclopedia of Mathematics and its Applications, Addison-Wesley Publishing Co., Reading, MA, 1981. Basic theory, With a foreword by Peter A. Carruthers.
[6] A. Bayliss and E. Turkel, *Radiation boundary conditions for wave-like equations*, Comm. Pure Appl. Math., 33 (1980), pp. 707–725.
[7] A. Bendali and P. Guillaume, *Non-reflecting boundary conditions for waveguides*, Math. Comp., 68 (1999), pp. 123–144.
[8] J.-P. Berenger, *A perfectly matched layer for the absorption of electromagnetic waves*, J. Comput. Phys., 114 (1994), pp. 185–200.
[9] Y. Boubendir, X. Antoine, and C. A. Geuzaine, *A non-overlapping quasi-optimal optimized Schwarz domain decomposition algorithm for the Helmholtz equation*, in Domain decomposition methods in science and engineering XX, vol. 91 of Lect. Notes Comput. Sci. Eng., Springer, Heidelberg, 2013, pp. 519–526.
[10] Z. Chen and X. Xiang, *A source transfer domain decomposition method for Helmholtz equations in unbounded domain*, SIAM J. Numer. Anal., 51 (2013), pp. 2331–2356.
[11] ———, *A source transfer domain decomposition method for Helmholtz equations in unbounded domain Part II: Extensions*, Numer. Math. Theory Methods Appl., 6 (2013), pp. 538–555.
[12] W. C. Chew and W. H. Weedon, *A 3D perfectly matched medium from modified Maxwell's equations with stretched coordinates*, Microwave and Optical Technology Letters, 7 (1994), p. 599 – 604.
[13] B. Engquist and A. Majda, *Radiation boundary conditions for acoustic and elastic wave calculations*, Comm. Pure Appl. Math., 32 (1979), pp. 314–358.
[14] B. Engquist and L. Ying, *Sweeping preconditioner for the Helmholtz equation: moving perfectly matched layers*, Multiscale Model. Simul., 9 (2011), pp. 686–710.
[15] G. J. Fix and S. P. Marin, *Variational methods for underwater acoustic problems*, J. Comput. Phys., 28 (1978), pp. 253–270.
[16] M. J. Gander, *Optimized Schwarz methods*, SIAM J. Numer. Anal., 44 (2006), pp. 699–731.
[17] M. J. Gander and H. Zhang, *A class of iterative solvers for the Helmholtz equation: factorizations, sweeping preconditioners, source transfer, single layer potentials, polarized traces, and optimized Schwarz methods*, SIAM Rev., 61 (2019), pp. 3–76.
[18] ———, *Schwarz methods by domain truncation*, Acta Numer., 31 (2022), pp. 1–134.
[19] S. D. Gedney, *An anisotropie perfectly matched layer-absorbing medium for the truncation of FDTD lattices*, IEEE Transactions on Antennas and Propagation, 44 (1996), p. 1630 – 1639.
[20] D. Givoli, *High-order local non-reflecting boundary conditions: A review*, Wave Motion, 39 (2004), p. 319 – 326.
[21] M. N. Guddati and K.-W. Lim, *Continued fraction absorbing boundary conditions for convex polygonal domains*, Internat. J. Numer. Methods Engrg., 66 (2006), pp. 949–977.
[22] M. N. Guddati and S. Thirunavukkarasu, *Improving the convergence of Schwarz methods for Helmholtz equation*, in Domain Decomposition Methods in Science and Engineering XX, Springer, 2013, pp. 199–206.
[23] T. Hagstrom, *On high-order radiation boundary conditions*, in Computational Wave Propagation, B. Engquist and G. A. Kriegsmann, eds., vol. 86 of The IMA Volumes in Mathematics and its Applications, Springer New York, 1997, pp. 1–21.
[24] ———, *Radiation boundary conditions for the numerical simulation of waves*, in Acta numerica, 1999, vol. 8 of Acta Numer., Cambridge Univ. Press, Cambridge, 1999, pp. 47–106.
[25] ———, *New results on absorbing layers and radiation boundary conditions*, in Topics in computational wave propagation, vol. 31 of Lect. Notes Comput. Sci. Eng., Springer, Berlin, 2003, pp. 1–42.
[26] T. Hagstrom and S. Kim, *Complete radiation boundary conditions for the Helmholtz equation I: waveguides*, Numer. Math., 141 (2019), pp. 917–966.
[27] ———, *Complete radiation boundary conditions for the Helmholtz equation II: domains with corners*, Numer. Math., 153 (2023), pp. 775–825.
[28] E. Hairer and G. Wanner, *Analysis by its history*, Undergraduate Texts in Mathematics, Springer-Verlag, New York, 2008. Corrected reprint of the 1996 original [MR1410751], Undergraduate Texts in Mathematics. Readings in Mathematics.
[29] M. Halla, T. Hohage, L. Nannen, and J. Schöberl, *Hardy space infinite elements for time harmonic wave equations with phase and group velocities of different signs*, Numer. Math., 133 (2016), pp. 103–139.
[30] M. Halla and L. Nannen, *Hardy space infinite elements for time-harmonic two-dimensional elastic waveguide problems*, Wave Motion, 59 (2015), pp. 94–110.
[31] P. Henrici, *Applied and computational complex analysis. Vol. 2*, Wiley-Interscience [John

Wiley & Sons], New York-London-Sydney, 1977. Special functions—integral transforms—asymptotics—continued fractions.
[32] T. Hohage and L. Nannen, *Hardy space infinite elements for scattering and resonance problems*, SIAM J. Numer. Anal., 47 (2009), pp. 972–996.
[33] T. Hohage, F. Schmidt, and L. Zschiedrich, *Solving time-harmonic scattering problems based on the pole condition. I. Theory*, SIAM J. Math. Anal., 35 (2003), pp. 183–210.
[34] D. Ingerman, V. Druskin, and L. Knizhnerman, *Optimal finite difference grids and rational approximations of the square root. I. Elliptic problems*, Comm. Pure Appl. Math., 53 (2000), pp. 1039–1066.
[35] F. Jarre and J. Stoer, *Optimalitätsbedingungen für allgemeine Optimierungsprobleme*, Springer Berlin Heidelberg, Berlin, Heidelberg, 2004, pp. 243–269.
[36] J. B. Keller and D. Givoli, *Exact nonreflecting boundary conditions*, J. Comput. Phys., 82 (1989), pp. 172–192.
[37] W. Murray and M. L. Overton, *A projected Lagrangian algorithm for nonlinear minimax optimization*, SIAM J. Sci. Statist. Comput., 1 (1980), pp. 345–370.
[38] L. Nannen and A. Schädle, *Hardy space infinite elements for Helmholtz-type problems with unbounded inhomogeneities*, Wave Motion, 48 (2011), pp. 116–129.
[39] D. Ruprecht, A. Schädle, and F. Schmidt, *Transparent boundary conditions based on the pole condition for time-dependent, two-dimensional problems*, Numer. Methods Partial Differential Equations, 29 (2013), pp. 1367–1390.
[40] D. Ruprecht, A. Schädle, F. Schmidt, and L. Zschiedrich, *Transparent boundary conditions for time-dependent problems*, SIAM J. Sci. Comput., 30 (2008), pp. 2358–2385.
[41] A. Schädle and L. Zschiedrich, *Additive Schwarz method for scattering problems using the PML method at interfaces*, in Domain decomposition methods in science and engineering XVI, vol. 55 of Lect. Notes Comput. Sci. Eng., Springer, Berlin, 2007, pp. 205–212.
[42] F. Schmidt, *An alternative derivation of the exact DtN-map on a circle*, Tech. Rep. SC-98-32, ZIB, Takustr. 7, 14195 Berlin, 1998.
[43] F. Schmidt, T. Hohage, R. Klose, A. Schädle, and L. Zschiedrich, *Pole condition: a numerical method for Helmholtz-type scattering problems with inhomogeneous exterior domain*, J. Comput. Appl. Math., 218 (2008), pp. 61–69.
[44] C. C. Stolk, *A rapidly converging domain decomposition method for the Helmholtz equation*, J. Comput. Phys., 241 (2013), pp. 240–252.
[45] A. Toselli, *Overlapping methods with perfectly matched layers for the solution of the Helmholtz equation*, in Eleventh International Conference on Domain Decomposition Methods, Citeseer, 1999, pp. 551–558.
[46] S. V. Tsynkov, *Numerical solution of problems on unbounded domains. a review*, Applied Numerical Mathematics, 27 (1998), p. 465 – 532.
[47] L. Zepeda-Núñez and L. Demanet, *The method of polarized traces for the 2D Helmholtz equation*, J. Comput. Phys., 308 (2016), pp. 347–388.